

See discussions, stats, and author profiles for this publication at: <https://www.researchgate.net/publication/231642951>

# Experimental and Theoretical Studies of Trimethylene Sulfide-Derived Nanostructures on p- and n-Type H-Silicon(100)-2 × 1

ARTICLE *in* THE JOURNAL OF PHYSICAL CHEMISTRY C · JULY 2007

Impact Factor: 4.77 · DOI: 10.1021/jp072011l

CITATIONS

23

READS

39

5 AUTHORS, INCLUDING:



**Gino DiLabio**

University of British Columbia - Okanagan

124 PUBLICATIONS 4,903 CITATIONS

SEE PROFILE



**Janik Zikovsky**

Thomson Reuters

17 PUBLICATIONS 328 CITATIONS

SEE PROFILE



**Jason L Pitters**

National Research Council Canada

54 PUBLICATIONS 745 CITATIONS

SEE PROFILE

Article

**Experimental and Theoretical Studies of Trimethylene  
Sulfide-Derived Nanostructures on p- and n-Type H-Silicon(100)-2 × 1**

Stanislav A. Dogel, Gino A. DiLabio, Janik Zikovsky, Jason L. Pitters, and Robert A. Wolkow

*J. Phys. Chem. C*, **2007**, 111 (32), 11965-11969 • DOI: 10.1021/jp072011I

Downloaded from <http://pubs.acs.org> on January 6, 2009

**More About This Article**

Additional resources and features associated with this article are available within the HTML version:

- Supporting Information
- Links to the 3 articles that cite this article, as of the time of this article download
- Access to high resolution figures
- Links to articles and content related to this article
- Copyright permission to reproduce figures and/or text from this article

[View the Full Text HTML](#)



**ACS Publications**  
High quality. High impact.

The Journal of Physical Chemistry C is published by the American Chemical Society.  
1155 Sixteenth Street N.W., Washington, DC 20036

# Experimental and Theoretical Studies of Trimethylene Sulfide-Derived Nanostructures on p- and n-Type H-Si(100)-2 × 1

Stanislav A. Dogel,<sup>†</sup> Gino A. DiLabio,<sup>\*,‡</sup> Janik Zikovsky,<sup>†</sup> Jason L. Pitters,<sup>‡</sup> and Robert A. Wolkow<sup>†</sup>

Department of Physics, University of Alberta, Edmonton, Alberta, Canada T6G 2G7, and National Institute for Nanotechnology, National Research Council of Canada, 11421 Saskatchewan Drive, Edmonton, Alberta, Canada T6G 2M9

Received: March 12, 2007

The nanoscale structuring of molecules on silicon surfaces is one approach for combining the tuneable properties of chemical species with the functionality of semiconductor materials. In this study, we report on the growth characteristics of trimethylene sulfide (TMS) on p- and n-type H-Si(100)-2 × 1. The nanostructures formed by TMS on either surface are indistinguishable by scanning tunneling microscopy (STM). However, high-resolution electron energy loss spectroscopy (HREELS) and modeling by density functional theory indicate that the molecular attachment mechanism differs with dopant type. Our results show that TMS adds to a surface silicon dangling bond through the formation of a Si-S bond on p-type silicon and through the formation of a Si-C bond on n-type silicon. In both cases, the added TMS undergoes ring opening following covalent bond formation with the surface. The different ring-opened radicals are able to abstract a hydrogen atom from one of two neighboring silicon dimers. The overall reaction produces TMS-derived nanostructures that grow via a square-wave pattern on the neighboring edges of two dimer rows.

## Introduction

The nanoscale structuring of molecules on silicon surfaces is one approach for combining the tuneable properties of chemical species with the functionality of semiconductor materials.<sup>1</sup> We demonstrated that styrene undergoes a radical-mediated, self-directed reaction on nominally hydrogen-terminated silicon(100)-2 × 1 surfaces, resulting in the formation of linear organic nanostructures.<sup>2</sup> This growth process is initiated by the addition of the styrene through its vinyl moiety to rare dangling bonds (DBs) on the surface. This addition results in the formation of a covalent Si-C bond and the concurrent formation of a carbon-centered radical. The carbon-centered radical (C<sup>•</sup>) then abstracts a hydrogen atom from a neighboring dimer on the silicon surface, thereby creating a new DB that is juxtaposed with the added molecule and is able to react with another styrene. Structures are formed by multiple, sequential reactions of this kind with no human intervention.

The arrangement of molecules within the organic nanostructures formed by this radical-mediated process depends upon the reconstruction of the silicon surface and the chemical structure (geometry) associated with the radical center following molecule addition. For the case of styrene on H-Si(100)-2 × 1, the anisotropy of the surface and the maximum distance, *d*, between the site of molecular attachment and the C<sup>•</sup> center causes the H abstraction to occur within the same dimer row as molecular addition (see ref 2). Thus, the styrene self-directed growth results in the formation of linear nanostructures along the dimer rows. The nanostructures derived from other molecules containing vinyl groups (vinylferrocene<sup>3</sup> and undecene<sup>4</sup>) and aldehyde groups (benzaldehyde and acetaldehyde)<sup>5</sup> display similar growth

characteristics, with single and/or double lines of molecules forming along the dimer rows.

Changes in *d* can substantially alter the configuration of the nanostructures that are formed. This property can be synthesized into the molecule to which the surface is exposed and therefore it is an important element in the rational design of organic nanostructures on silicon. For example, we showed that cyclopropylmethyl ketone undergoes a ring-opening rearrangement upon attachment to the surface.<sup>6</sup> Because *d* for the ring-opened species is variable and has a large maximum value, the growth resulted in nanostructures with random and irregular configurations. More recently, work by Kawai's group showed that increasing *d* through the use of allyl mercaptan (ALM) results in linear nanostructure formation exclusively across dimer rows rather than in the dimer row direction as in the styrene case.<sup>7</sup> They used the difference in styrene and ALM growth characteristics to create L-shaped structures on silicon, although building the structures into the second dimension required the manual creation of new growth initiation sites.<sup>7b</sup>

As part of our effort to explore new molecular building blocks for nanostructure formation, we report in this work the growth characteristics of trimethylene sulfide (TMS) on p- and n-type H-Si(100)-2 × 1 as determined by scanning tunneling microscopy (STM), high-resolution electron energy loss spectroscopy (HREELS), and modeling by density functional theory. One of our initial expectations was that TMS would react with the silicon DB on an n-type crystal through the formation of a Si-C bond with concomitant ring-opening. This would result in an intermediate species identical to that associated with ALM line growth and therefore provide an alternative approach to line growth in the perpendicular-to-dimer-row direction. Our results, however, show that TMS produces structures that grow along dimer rows. Some mechanistic insights for TMS line growth obtained from HREELS and modeling are presented.

\* Corresponding author. E-mail: Gino.DiLabio@nrc.ca. Tel: +1-780-641-1729. Fax: +1-780-641-1601.

<sup>†</sup> University of Alberta.

<sup>‡</sup> NRC-NINT.

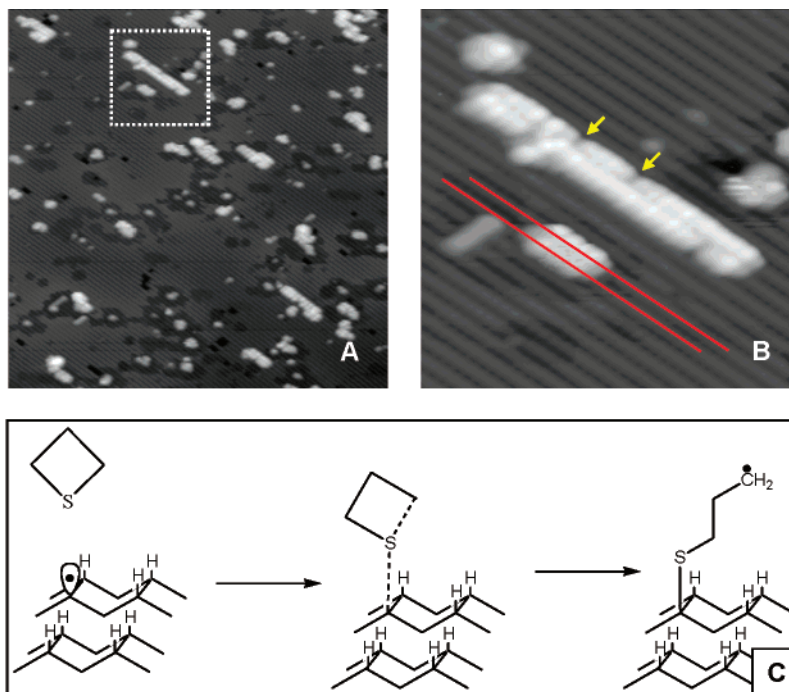


**Figure 1.** (A) STM image ( $50 \times 50 \text{ nm}^2$ , sample bias  $-3.0 \text{ V}$ , tunneling current  $0.06 \text{ nA}$ ) of 200 L of TMS on p-type medium doped H-Si(100)- $2 \times 1$ . The selected area is magnified in panel B, with lines indicating the centers of two dimer rows. The yellow arrows indicate two missing molecule defects. (C) Reaction mechanism for the addition of TMS on p-type H-Si(100)- $2 \times 1$ .

### Experimental and Computational Methods

Scanning tunneling microscopy (STM 1, Omicron, Germany) and high-resolution electron energy loss spectroscopy (LK 3000, LK Technology, USA) experiments were carried out in the same UHV system with a base pressure below  $10^{-10}$  Torr. Samples cut from arsenic doped ( $0.08\text{--}0.1 \text{ } \Omega\cdot\text{cm}$ ) and boron-doped ( $0.01\text{--}0.03 \text{ } \Omega\cdot\text{cm}$ ) Si(100) wafers (Virginia Semiconductors, USA) were degassed for 10–15 h at 870 K. The native oxide layer was removed by repeated flashing up to 1520 K with a base pressure remaining below  $2 \times 10^{-10}$  Torr. Hydrogen termination of the surfaces was performed by heating the clean surfaces to 570 K during exposure to atomic hydrogen (120 s at  $10^{-6}$  Torr) generated at a hot tungsten filament.<sup>8</sup>

TMS (Aldrich, 97%) was purified by several freeze–pump–thaw cycles prior to dosing through a variable leak valve. The dosing was performed in an attached preparation chamber at room temperature. The samples were then transferred either to the STM or HREELS chambers for analysis. STM measurements were performed at room temperature and HREELS experiments were conducted at 110–140 K.

HREELS was performed in the specular scattering geometry ( $60^\circ$  with respect to surface normal) at incident energy 6.3 eV and a resolution of 3.0 meV in the straight-through geometry. Since the intensity of the energy losses are coverage-dependent, we used a higher dosing level for HREELS in comparison to STM experiments in order to obtain better signal-to-noise ratios. The contributions due to the thermal excitation of low-energy plasmons were removed from HREEL spectra using a procedure previously described.<sup>9</sup> This approach helps to reveal loss peaks in the low-energy region. Animation of calculated vibrations was used to assist in the assignment of measured HREELS peaks (vide infra).

All calculations were performed using the Gaussian-03 suite of programs.<sup>10</sup> The reactions involving the addition of TMS on silicon were modeled using a two-dimer,  $\text{Si}_{15}\text{H}_{19}$ , silicon cluster representing a  $2 \times 1$  hydrogen-terminated silicon(100) surface with a single surface dangling bond. This cluster has three

surface hydrogen atoms and the remaining 16 H atoms cap the dangling silicon back-bonds. The structures of the transition states and the addition products were obtained using the B3P86<sup>11</sup>/6-31+G(d,p) level of theory. A similar model approach using B3P86/6-31G(d) geometry optimizations has been shown to accurately predict substituent effects on bond dissociation enthalpies.<sup>12</sup> The energy barriers associated with the hydrogen atom transfer reactions were modeled with B3P86/6-31G(d) on a  $\text{Si}_{40}\text{H}_{51}$  cluster (two rows of three dimers) in which the positions of the capping H atoms were frozen. The energy maxima along the H-transfer coordinate was determined by incrementing the distance between the transferring H and the radical center ( $\text{S}^\bullet$  or  $\text{C}^\bullet$ ) by 0.05 Å while the positions of the Si and non-capping H atoms were allowed to relax.

Additional calculations were performed in order to obtain IR and Raman spectra of TMS on silicon. For these calculations, we used BLYP<sup>13</sup>/6-31G(d) on a two dimer cluster like that described above. For the spectra calculations, however, we capped the Si back-bonds of the cluster with Si quantum capping potentials (QCPs).<sup>14</sup> In doing so, the computed spectra are free of artifact Si–H and  $\text{SiH}_2$  peaks that would be obtained if a hydrogen-capped cluster were used. This approach was described in detail elsewhere.<sup>9</sup>

### Results and Discussion

**Reaction of TMS on p-type H-Si(100)- $2 \times 1$ .** Figure 1A shows a STM image of organic nanostructures formed after dosing 200 L of TMS on p-type H-Si(100). The nanostructures are approximately linear and appear to be composed of two lines of molecules. Close examination of the STM image (Figure 1B) reveals that the two lines are not on a single dimer row but the structures grew along the neighboring edges of two adjacent dimer rows. Various other TMS features found in Figure 1A appear to be the result of growth across a number of dimer rows. Our experimental procedure did not allow for registered before-and-after dose imaging, and therefore it is not possible to discern the detailed growth mechanism of those features. It is possible

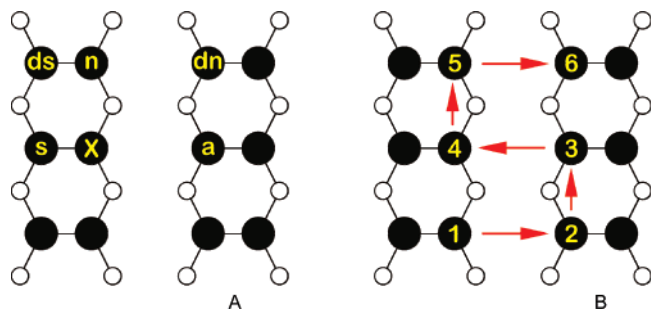


**Figure 2.** Schematics showing a top-down view of two rows of three dimers of H-Si(100)-2  $\times$  1. The large, dark circles represent surface Si atoms capped by H atoms. The smaller, open circles represent the silicon atoms of the next layer below the surface. (A) The X denotes a surface DB to which TMS attaches. The remaining letters represent the various H-abstraction sites: a = across, n = next dimer, s = same, dn = diagonal next row, ds = diagonal same row. (B) Sequence of multiple TMS attachment events indicated by the numbers. The arrows illustrate the proposed "square-wave" growth pattern for TMS.

that some features involving multiple rows formed as a result of several lines having grown to a common termination point.

Our calculations point to a most probable growth mechanism for the double lines, which is illustrated in Figure 1C. A weakly stabilizing dative interaction occurs between a nominally neutral surface DB and a sulfur lone-pair of electrons from TMS. A formal Si-S covalent bond then forms concurrently with the scission of an S-C TMS bond, which leads to a ring-opened, carbon-centered radical attached to the surface. The barrier height computed for this process is less than the dative-bond energy. The overall addition process is calculated to be exoergic by 18 kcal/mol. Additional calculations were performed to explore the possibility of the addition of TMS through the formation of a Si-C bond. A reaction path for this mechanism was located and the associated barrier was computed to be 16.1 kcal/mol. Therefore, the addition of TMS through a C atom is highly disfavored relative to addition through a S atom.<sup>15</sup>

The maximum length of the radical is roughly 4.2 Å, a  $d$  value that potentially allows the C $\cdot$  to abstract a hydrogen atom from any one of a number of nearby sites (see Figure 2A). The results of our calculations indicate that the lowest energy barrier ( $E_{\text{bar}}$ ) to abstraction (2.6 kcal/mol) involves the H on the next dimer row, immediately across (site a) from the point of TMS attachment (site X). Abstraction of H from the next dimer in the same row and on the same side of the row as the attached TMS (site n) has a computed  $E_{\text{bar}}$  of 2.9 kcal/mol. Abstraction from the same dimer (site s) has a computed  $E_{\text{bar}}$  of 3.5 kcal/mol but requires that the attached radical overcomes one internal ethane-type barrier to rotation in order for the radical center to be properly positioned for abstraction. Abstractions from the "diagonal" site on the same row (site ds) or on the neighboring row (site dn) have higher computed barriers (8.4 and 9.9 kcal/mol, respectively) and are much less likely to occur. The overall calculated reaction energy including TMS addition through the S atom and abstraction of a nearby H is -43.0 kcal/mol, relative to separated reactants.<sup>16</sup> This large exoergicity is mostly due to the formation of a strong C-H  $\sigma$ -bond upon H-abstraction from the surface.

The computational results suggest that the growth of TMS on p-type silicon is likely to occur by a "square-wave" pattern (illustrated in Figure 2B) as follows: (i) attachment of TMS to a surface DB site with concomitant ring-opening; (ii) H abstraction from the dimer in the next dimer row, immediately across from the TMS attachment point; (iii) addition of a second

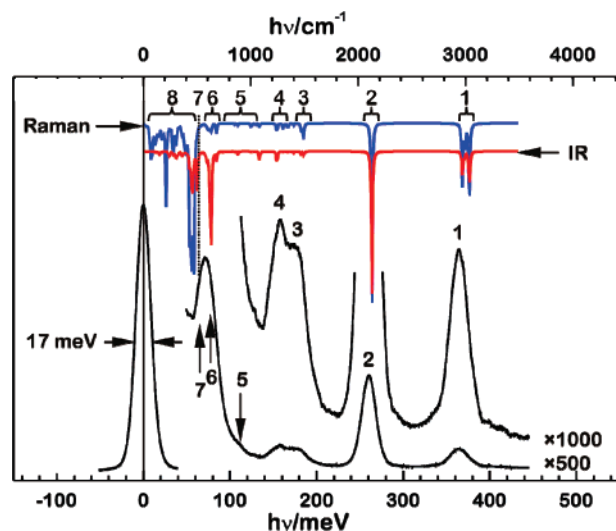


**Figure 3.** HREEL spectrum of 200 L TMS on the p-type medium doped H-Si(100)-2  $\times$  1 taken at  $\sim$ 110 K (black) and results of calculations (IR, red; Raman, blue). Peaks assignments are made as follows (experimental/calculated range in  $\text{cm}^{-1}$ ): (1) (2900/2968–3042) CH<sub>2</sub> and CH<sub>3</sub> symmetric and asymmetric stretches, (2) (2090/2125) Si-H stretches, (3) (1440/1345–1502) CH<sub>2</sub> scissors and CH<sub>3</sub> s-deformations, (4) (1254/1047–1302) CH<sub>2</sub> wags and twists and CH<sub>3</sub> s-deformations, (5) (900/1004,879) C-C stretches and CH<sub>2</sub> and CH<sub>3</sub> deformations, (6) (572/587–633) Si-H bends (dotted line) and (–/681) C-S stretch, (7) (500/500) Si-S stretch (see text for additional details of assignment), (8) (–/50–470) calculated cluster modes.

TMS to the DB on the site a which is formed after the abstraction in point ii, in the same fashion as described in point i; (iv) abstraction of a H atom from the next dimer in the same row and on the same side as the added TMS in point iii; (v) addition of a third TMS on the new DB site; (vi) abstraction of a H atom from the "across" site as in point ii. The square-wave growth of TMS is analogous to that which occurs with benzaldehyde on silicon,<sup>5</sup> except that the former involves two dimer rows whereas the latter is limited to only one dimer row because of a smaller  $d$  value.

A closer look at Figure 1B shows that the double line appears to have some missing molecules (indicated by yellow arrows). This is consistent with the small difference in computed barrier heights for abstractions from the "across" and "next" sites: If an additional "next" abstraction step occurs in the place of an "across" abstraction, growth would continue in the square-wave pattern but with a missing molecule defect in the organic nanostructure.

Support for the addition reaction occurring via the formation of a Si-S bond is provided by the results of HREELS experiments and cluster calculations. Figure 3 shows the measured spectra for the addition of TMS on p-type, medium doped silicon. Also shown in Figure 3 are the calculated IR and Raman spectra for the addition product for the reaction of TMS on a neutral silicon cluster in which a Si-S bond is formed. The model used for simulating the vibration spectra is that which represents the TMS having undergone the addition and subsequent H-abstraction reactions. Figure 3 shows a number of peaks for which assignments are given in the caption. The peak of particular interest in connection with the addition mechanism occurs near 500  $\text{cm}^{-1}$ , in the region where our calculations predict Si-S (labeled 7) stretching to occur.<sup>17</sup> A prominent Si-H bending peak is also expected in this region (labeled 6). Since the measured peak in our spectrum is broadened by ca. 20% with respect to the elastic peak and shifted to lower energy than that expected for the Si-H bend, it is



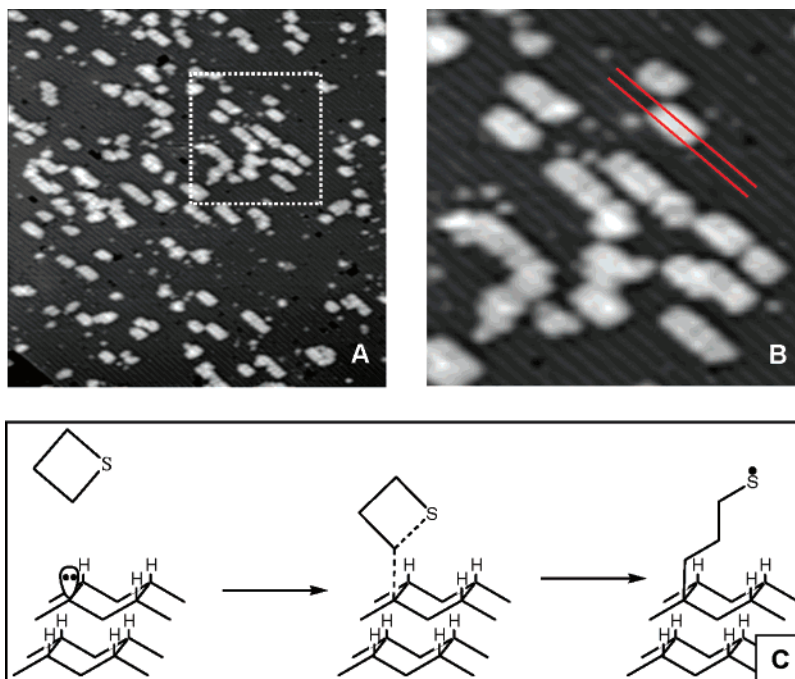


**Figure 4.** (A) STM image ( $50 \times 50 \text{ nm}^2$ , sample bias  $-3.0 \text{ V}$ , tunneling current  $0.05 \text{ nA}$ ) of 80 L of TMS on the n-type medium doped H-Si(100)- $2 \times 1$ . The selected area is magnified in panel B (lines mark the center of the dimer rows). (C) Reaction mechanism for the addition of TMS on n-type H-Si(100)- $2 \times 1$ .

very likely a convolution of the Si-H bend and Si-S stretch peaks.

It is important to note that if the attachment of TMS occurred through a Si-C bond, a S-H stretching peak would be expected in the region near  $2500 \text{ cm}^{-1}$  (vide infra). However, no S-H peak is observed in the spectrum. The presence of the Si-S peak and the absence of a S-H peak support our proposed mechanism that TMS adds to p-type silicon through a Si-S bond.

**Reaction of TMS on n-type H-Si(100)- $2 \times 1$ .** Figure 4A shows a STM image of organic nanostructures formed after dosing 80 L of TMS on n-type H-Si(100). The image does not reveal any substantial differences between the nanostructures formed by TMS on n-type or p-type silicon (cf. Figure 1). As in the case of TMS growth on p-type silicon, the nanostructures formed are composed of double-lines of molecules on two dimer rows. In some instances, features appear to involve more than two dimer rows but we are unable to conclude whether these originate from a single DB or from multiple growth-initiating DBs. An enlarged image of a double-line nanostructure feature is provided in Figure 4B.

In our STM and HREELS experiments, the surface DB density on the silicon is low enough relative to the dopant density that the DBs are negatively charged. TMS addition cannot occur through the S atom because of anion-lone-pair repulsion. This expectation is supported by the result of our calculations, which show that the potential energy along the reaction coordinate associated with the approach of the S atom of TMS to a negatively charged DB on silicon is completely repulsive.<sup>19</sup> However, addition can occur via the nucleophilic attack of a TMS C atom by the negatively charged, surface DB (as shown in Figure 4C). For this case, the calculations predict a weak association complex between the anionic silicon cluster and TMS. Addition occurs through the formation of a Si-C bond, a viable process with a calculated barrier height of 14.9 kcal/mol. The negatively charged, ring-opened addition product is stable by 11.6 kcal/mol relative to the pre-reaction complex. We expect that during or shortly after the addition, the negative

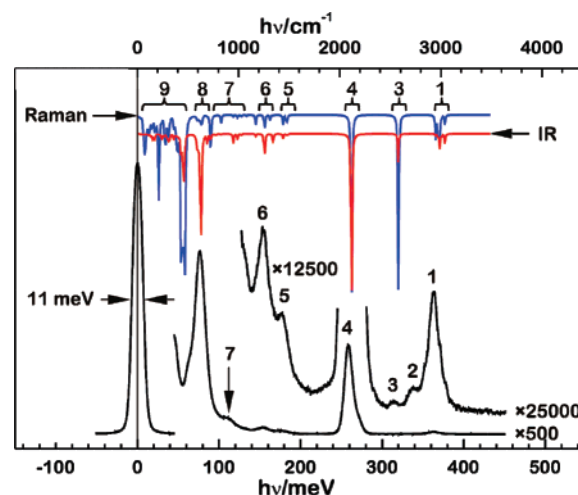


**Figure 5.** HREEL spectrum of 180 L of TMS on the n-type medium doped H-Si(100)- $2 \times 1$  taken at  $\sim 130 \text{ K}$  (black) and results of calculations (IR, red; Raman, blue). Peaks assignments are made as follows (experimental/calculated range in  $\text{cm}^{-1}$ ): (1) (2920/2948–3041)  $\text{CH}_2$  symmetric and asymmetric stretches, (2) unidentified—see text for details, (3) (2535/2580) S-H stretch, (4) (2083/2115) Si-H stretches, (5) (1440/1440–1489)  $\text{CH}_2$  scissors, (6) (1250/1078–1342)  $\text{CH}_2$  wags and twists, (7) (900/687–987) C-C stretches,  $\text{CH}_2$  wags and (-/1026,724) CSH bends, (8) (-/643) Si-C and C-S stretches, (615/586–634) Si-H bends, (9) (-/50–470) calculated cluster modes.

charge will go into the bulk silicon and leave behind a formally neutral, ring-open system with an unpaired electron residing on the S.<sup>20,21,22</sup>

The length of the radical attached to the surface through the C atom is about  $4.2 \text{ \AA}$  (the same as that attached through the S atom) and again passivation by H-abstraction from one of a number of accessible sites is possible. Our calculations predict that abstraction is most likely to occur from the next row (Figure 2A, site a), from the dimer immediately across from the point of TMS attachment ( $E_{\text{bar}} = 2.9 \text{ kcal/mol}$ ) and from the next dimer in the same row and on the same side of the

row (site n) as the attached TMS ( $E_{\text{bar}} = 4.1$  kcal/mol). Abstraction of H from the same dimer to which attachment occurs (site s) has a computed  $E_{\text{bar}}$  of 5.6 kcal/mol and requires an internal rotation in order to establish the transition state geometry. The time constants for the latter two abstractions are roughly one and 2 orders of magnitude, respectively, slower than that associated with abstraction from the “across” site. Abstractions from the site ds ( $E_{\text{bar}} = 7.5$  kcal/mol) or site nd (13.4 kcal/mol) are not expected to occur. The overall calculated reaction energy including TMS addition through a C atom and abstraction of a nearby H is  $-25.1$  kcal/mol, relative to separated reactants.<sup>16</sup> The lower exoergicity of this reaction compared to that on p-type silicon reflects the fact that the S–H and Si–H bond strengths are comparable.

The computational data suggest that nanostructure formation of TMS on n-type H–Si(100)-2 × 1, like on p-type H–Si(100)-2 × 1, occurs by the “square-wave” pattern described above (see Figure 2B) and involves two adjacent dimer rows. This prediction for the dominant growth mechanism is supported by the STM observations.

The measured HREEL spectrum for TMS on n-type H–Si(100)-2 × 1 is shown in Figure 5. Also shown in the Figure are the calculated IR and Raman spectra for the H-passivated, TMS-derived addition product in which a Si–C bond is present. Peak assignments are given in the caption. Not surprisingly, the spectra shown in the Figure have many features in common with those shown in Figure 3. However, there are two measured peaks, labeled 2 and 3, that are unique to the measured spectrum shown in Figure 5. We are able to readily identify peak 3 at 2523 cm<sup>-1</sup> (calculated 2580 cm<sup>-1</sup>) as being due to S–H stretching.<sup>23</sup> The presence of this peak provides support for our suggestion that TMS adds to n-type H–Si(100)-2 × 1 through the formation of a Si–C bond. This addition results in the presence of a –SH group on the attached species, which is present following the passivation of the sulfur radical intermediate via a H abstraction process. We were unable to identify any molecular vibrations that could lead to peak 2 near 2750 cm<sup>-1</sup>.<sup>24</sup>

Our proposed mechanism for the reaction of TMS on n-type H–Si(100)-2 × 1 conflicts to some extent with the mechanism for perpendicular-to-dimer row ALM line growth offered by Hossain et al.<sup>7b</sup> (see Figure 3 of ref 7b). Both proposed mechanisms involve the formation of a common sulfur-centered radical of the form  $\text{surface-Si-CH}_2\text{-CH}_2\text{-CH}_2\text{-S}^\bullet$ . However, in the present case, only double-line growth along dimer rows is observed. We emphasize that our calculations reveal that the barriers to H-abstraction by the attached radical intermediate in question are extremely small and cannot lead to the growth observed by Hossain et al.<sup>25</sup> Therefore, an alternative mechanism must be responsible to the perpendicular-to-line growth of ALM.

## Concluding Remarks

Using STM, we observed the formation of nanostructures of TMS on p- and n-type H–Si(100)-2 × 1 that are nominally composed of two adjacent lines of molecules on two silicon dimer rows of the substrate. The results of calculations indicate that the growth mechanism on both types of doped Si follows a “square-wave” pattern.

The vibration spectra obtained by HREELS and modeled computationally indicate that the mode of attachment of TMS depends on the whether the silicon is p-type or n-type: For p-type H–Si(100)-2 × 1, the attachment of TMS occurs through the formation of a Si–S bond and for n-type H–Si(100)-2 × 1, the attachment of TMS occurs through the formation of a Si–C bond. These results illustrate a simple example of dopant-mediated chemistry.

**Acknowledgment.** G.A.D. thanks the Centre for Excellence in Integrated Nanotools (University of Alberta) for access to computational facilities. We are grateful to iCORE, CIAR and NSERC for financial support. We are very grateful to Dr. Baseer Haider for performing ALM line growth experiments.

## References and Notes

- (1) Piva, P. G.; DiLabio, G. A.; Pitters, J. L.; Zikovsky, J.; Rezek, M.; Dogel, S.; Hofer, W. A.; Wolkow, R. A. *Nature* **2005**, *435*, 658–661.
- (2) Lopinski, G. P.; Wayner, D. D. M.; Wolkow, R. A. *Nature* **2000**, *406*, 48–51.
- (3) Kruse, P.; Johnson, E. R.; DiLabio, G. A.; Wolkow, R. A. *Nano Lett.* **2002**, *2*, 807–810.
- (4) DiLabio, G. A.; Piva, P. G.; Kruse, P.; Wolkow, R. A. *J. Am. Chem. Soc.* **2004**, *126*, 16048–16050.
- (5) Pitters, J. L.; Dogel, I.; DiLabio, G. A.; Wolkow, R. A. *J. Phys. Chem. B* **2006**, *110*, 2159–2163.
- (6) Tong, X.; DiLabio, G. A.; Clarkin, O. J.; Wolkow, R. A. *Nano Lett.* **2004**, *4*, 357–360.
- (7) a) Hossain, M. Z.; Kato, H. S.; Kawai, M. *J. Phys. Chem. B* **2005**, *109*, 23129–23133. b) Hossain, M. Z.; Kato, H. S.; Kawai, M. *J. Am. Chem. Soc.* **2005**, *127*, 15030–15031.
- (8) Boland, J. J. *Surf. Sci.* **1992**, *261*, 17–28.
- (9) DiLabio, G. A.; Dogel, S. A.; Wolkow, R. A. *Surf. Sci.* **2006**, *600*, L209–L213.
- (10) Frisch, M. J.; Trucks, G. W.; Schlegel, H. B.; Scuseria, G. E.; Robb, M. A.; Cheeseman, J. R.; Montgomery, J. A., Jr.; Vreven, T.; Kudin, K. N.; Burant, J. C.; Millam, J. M.; Iyengar, S. S.; Tomasi, J.; Barone, V.; Mennucci, B.; Cossi, M.; Scalmani, G.; Rega, N.; Petersson, G. A.; Nakatsuji, H.; Hada, M.; Ehara, M.; Toyota, K.; Fukuda, R.; Hasegawa, J.; Ishida, M.; Nakajima, T.; Honda, Y.; Kitao, O.; Nakai, H.; Klene, M.; Li, X.; Knox, J. E.; Hratchian, H. P.; Cross, J. B.; Adamo, C.; Jaramillo, J.; Gomperts, R.; Stratmann, R. E.; Yazyev, O.; Austin, A. J.; Cammi, R.; Pomelli, C.; Ochterski, J. W.; Ayala, P. Y.; Morokuma, K.; Voth, G. A.; Salvador, P.; Dannenberg, J. J.; Zakrzewski, V. G.; Dapprich, S.; Daniels, A. D.; Strain, M. C.; Farkas, O.; Malick, D. K.; Rabuck, A. D.; Raghavachari, K.; Foresman, J. B.; Ortiz, J. V.; Cui, Q.; Baboul, A. G.; Clifford, S.; Cioslowski, J.; Stefanov, B. B.; Liu, G.; Liashenko, A.; Piskorz, P.; Komaromi, I.; Martin, R. L.; Fox, D. J.; Keith, T.; Al-Laham, M. A.; Peng, C. Y.; Nanayakkara, A.; Challacombe, M.; Gill, P. M. W.; Johnson, B.; Chen, W.; Wong, M. W.; Gonzalez, C.; Pople, J. A. *Gaussian 03*, revision C.02; Gaussian, Inc.: Pittsburgh, 2003.
- (11) (a) Becke, A. D. *J. Chem. Phys.* **1993**, *98*, 5648–5652. (b) Perdew, J. P. *Phys. Rev. B* **1986**, *33*, 8822–8824.
- (12) Johnson, E. R.; Clarkin, O. J.; DiLabio, G. A. *J. Phys. Chem. A* **2003**, *107*, 9953–9963.
- (13) (a) Becke, A. D. *Phys. Rev. A* **1988**, *38*, 3098–3100. (b) Lee, C.; Yang, W.; Parr, R. G. *Phys. Rev. B* **1988**, *37*, 785–789.
- (14) DiLabio, G. A.; Wolkow, R. A.; Johnson, E. R. *J. Chem. Phys.* **2005**, *122*, 044708.
- (15) If the addition of TMS could be accomplished via the formation of a S–C bond, our calculation indicate that the exothermicity would be  $-19.1$  kcal/mol.
- (16) The overall reaction energy is essentially independent of the site from which H is abstracted.
- (17) Calculations on  $(\text{CH}_3)_3\text{Si-SC}_3\text{H}_8$  predict the Si–S stretch at 550 cm<sup>-1</sup>, in agreement with gas-phase experimental data.<sup>18</sup>
- (18) Fehér, F.; Goller, H. Z. *Naturforsch.* **1970**, *25b*, 250–252.
- (19) These calculations used a silicon cluster with a single DB and a formal negative charge. Additional calculations were performed in which a phosphorus dopant atom was incorporated into the cluster containing one surface DB. In this case, the cluster is formally neutral and the surface DB has a lone-pair of electrons. The potential energy curve associated with the reaction coordinate in question is also completely repulsive in this case.
- (20) This process cannot be adequately modeled with the techniques used in this work. However, the electron affinity of  $\text{RS}^\bullet$  is ca. 45 kcal/mol<sup>21</sup> and the conduction band of H–Si(100) lies ca. 92 kcal/mol below the vacuum level.<sup>22</sup> Therefore, the electron transfer from  $\text{RS}^-$  to the silicon is highly exothermic.
- (21) Berkowitz, J.; Ellison, G. B.; Gutman, D. *J. Phys. Chem.* **1994**, *98*, 2744–2765.
- (22) Sze, S. M. *The Physics of Semiconductor Devices*. John Wiley and Sons, Canada 1981.
- (23) Bellamy, L. J. *The Infra-red Spectra of Complex Molecules*; Chapman and Hill: London, 1975.
- (24) We do not believe that this peak is a multiple harmonic or a combination of different modes from the 800–1600 cm<sup>-1</sup> region, largely because no such phenomenon is observed in the spectra for the molecule on p-type silicon.
- (25) We have verified that ALM does indeed growth in the perpendicular-to-row direction, as demonstrated in ref 7.